Astha Chauhan and Rajan Arora*

Solution of the Riemann problem for an ideal polytropic dusty gas in magnetogasdynamics

https://doi.org/10.1515/zna-2019-0381 Received December 30, 2019; accepted March 17, 2020; published online May 6, 2020

Abstract: The main aim of this paper is, to obtain the analytical solution of the Riemann problem for a quasi-linear system of equations, which describe the one-dimensional unsteady flow of an ideal polytropic dusty gas in magnetogasdynamics without any restriction on the initial data. By using the Rankine-Hugoniot (R-H) and Lax conditions, the explicit expressions of elementary wave solutions (i. e., shock waves, simple waves and contact discontinuities) are derived. In the flow field, the velocity and density distributions for the compressive and rarefaction waves are discussed and shown graphically. It is also shown how the presence of small solid particles and magnetic field affect the velocity and density across the elementary waves. It is an interesting fact about this study that the results obtained for the Riemann problem are in closed form.

Keywords: contact discontinuity; dusty gas; magnetogasdynamics; rarefaction wave; Riemann problem; shock wave.

1 Introduction

In recent years, the solutions of Riemann problem for a system of conservation laws have grabbed the undivided attention of the researchers from the theoretical and numerical points of view in real gas flow, gas dynamics, magnetogasdynamics, shallow water flow, etc. In the case of the Euler equations, the Riemann problem corresponds to the so-called shock-tube problem, a fundamental physical problem in gas dynamics. One can go through the book [1] for its detailed discussion. The Riemann solution

Astha Chauhan: Department of Applied Science and Engineering, Indian Institute of Technology, Roorkee, India, E-mail: asthaiitr1@gmail.com achauhan1@as.iitr.ac.in. https://orcid.org/0000-0002-8995-2336

consists of three waves with single contact discontinuity as the middle one and the remaining two are shock or rarefaction waves. All the features of the solution of the Riemann problem such as shock waves, rarefaction waves and contact discontinuity appear in the form of characteristics. Therefore, it is convenient for the researchers/readers to understand the conservation form of Euler equations. The solution of the Riemann problem gives an idea of the wave structure of a system of non-linear hyperbolic differential equations. In recent years, the solutions of Riemann problem in gas dynamics have been obtained extensively by many researchers [2-4]. Lax [5] obtained the solution of the Riemann problem for the case when the difference between the initial states V_r and V_l , $||V_l - V_r||$ is sufficiently small, where V_r and V_l are the vectors of conserved variables to the right and left of x = 0 separated by a discontinuity at x = 0, respectively. Dafermos [6] established the existence of the solutions of the Riemann problem for a hyperbolic system of conservation laws by the viscosity method. Giacomazzo and Rezzolla [7], and Romero et al. [8] determined the exact solutions of the Riemann problem in magnetohydrodynamics. Ambika and Radha [9] solved the Riemann problem in a non-ideal gas. They have determined the explicit form of solutions of shock and rarefaction waves, and also derived the necessary and sufficient conditions on the initial data from which existence and uniqueness of the solution for shocks and rarefaction waves are determined. Recently, Gupta et al. [10] studied the Riemann problem in magnetogasdynamics for a nonideal polytropic gas and derived the explicit form of solutions of shock waves, simple waves and contact discontinuity. The effects of non-idealness and dusty gas particles on the compressive and rarefaction waves are discussed by them. Wang [11] studied the Riemann problem for generalized Chaplygin gas dynamics. The stability of the Riemann solutions with respect to the initial data is also discussed by him. Bernetti et al. [12] studied the Riemann problem for the shallow water equations with a piecewise constant bottom geometry and obtained the self-similar solution. Uniqueness of the solution is also discussed by them. Shen [13] solved the Riemann problem for Chaplygin gas dynamics with a Coulomb-like friction term. He derived the generalized R-H conditions for delta shock wave and shown that in Riemann solutions, the delta shock wave

^{*}Corresponding author: Rajan Arora, Department of Applied Science and Engineering, Indian Institute of Technology, Roorkee, India, E-mail: rajan.arora@as.iitr.ac.in

appears in certain situations. Zeidan et al. [14] proposed a new model and a solution method for two-phase two-fluid compressible flows; the key ingredient of the scheme is the solution of the Riemann problem. Two-phase flow is seen in a broad range of applications and encompasses many different physical processes. As regard to the numerical and analytical approaches for the simulation of two-phase flow equations, there are several methods from different perspectives to simulate two-phase flow problems. There have been reasonably successful attempts to use approximate Riemann solvers for two-phase flow equations. For the details of these methods and Riemann solvers, we refer the readers to the recent papers [15–20].

Understanding the influence of solid particles on the propagation phenomena of waves and the resulting flow field is of great importance for solving many engineering problems in the field of astrophysics and space science research. The study of Riemann problem for the fluid flow containing solid particles is a topic of great interest due to its many applications in lunar ash flow, nozzle flow, interstellar masses, volcanic explosions, underground explosions and in many other fields [21–23]. When a shock wave is propagated through a gas which contains a considerable amount of dust, the pressure, the temperature and the entropy change across the shock, and the other features of the flow differ greatly from those which arise when the shock passes through a dust-free gas. The flow field, that develops when a moving shock wave hits a twophase medium of gas and particles, has a close practical relation to industrial applications (e.g., solid rocket engine in which aluminum particles are used to reduce the vibration due to instability) as well as industrial accidents such as explosions in coalmines and grain elevators. Therefore, a successful prediction of the behavior of shock waves in a two-phase medium of gas and solid particles is very crucial and imperative for the successful design and operation of rocket nozzles and energy conversion systems. Dusty gas is a mixture of gas and small solid particles, where solid particles occupy less than 5% of the total volume. When the speed of fluid is very high, the small solid particles behave like a pseudo fluid [24]. There are many research articles related to the study of shock wave propagation in a dusty gas (see Refs. [25–27]). Chadha and Jena [28] studied the effects of dust particles on the propagation of waves in a non-ideal gas. They have obtained the shock trajectory with the effects of Van der Waals excluded volume and dust particles. Recently, Chauhan and Arora [29] have determined the solutions of strong shock waves for cylindrically symmetric flow in a non-ideal dusty gas with the inclusion of axial magnetic field. Nath et al. [30] studied the Riemann problem for an ideal

polytropic gas with dust particles. The study of magnetogasdymamics is a topic of great interest from the mathematical and physical points of view as it has many applications in the field of engineering physics, nuclear science, astrophysics, etc [31–34]. Shekhar and Sharma [35] obtained the solution of Riemann problem in an ideal magnetogasdynamic flow under the simplified assumption. This study is mainly concerned with the Riemann problem in a polytropic dusty gas for one-dimensional unsteady flow with the effect of transverse magnetic field. The dusty gas is a pure perfect gas that is contaminated by small solid particles and not as a mixture of two perfect gases. The solid particles are continuously distributed in the perfect gas and, in their totality are referred to as dust. It is assumed that the dust particles are highly dispersed in the gas phase such that the dusty gas can be considered as a continuous medium. It is also assumed that the equilibrium flow condition is maintained in the flow field, and that the viscous stress and heat conduction of the mixture is negligible. Here, we consider a single fluid model for a dusty gas in magnetogasdynamics. This system is more complex than the corresponding Riemann problem for the Euler equations in ordinary gas dynamics. The main motivation to work on magnetogasdynamics with dust particles is its application in Astrophysics as dusty plasmas are common in astrophysical environments; examples range from the interstellar medium to cometary tails and planetary ring system. The paper aims to provide an explicit solution to the Riemann problem for the one-dimensional Euler equations for dusty gas flow. We have compared/contrasted the nature of the solution in an ordinary gas dynamics/magnetogasdynamics and the dusty gas flow case.

The rest of the paper is summarized as follows: In Section 1, a brief introduction is presented about the Riemann problem in gas dynamics. In Section 2, the governing equations of motion describing the one-dimensional unsteady planar flow of an ideal polytropic dusty gas with the presence of transverse magnetic field are introduced. In Section 3, the mathematical form of Riemann problem is presented and the generalized Riemann invariants are determined. The explicit formulas for the 1-shock curve and the 3-shock curve are derived by using the jump conditions in Section 4. Section 6 is about simple waves or rarefaction waves. The explicit formulas for 1-rarefaction waves and 3rarefaction waves are derived in Section 5. Section 6 is about contact discontinuities. The results of this paper are discussed in Section 7. The graphical representations of compressive and rarefaction wave for 1-shock and 3-shock are also presented. The effects of dusty gas particles and magnetic field are shown in Section 7. In section 8, a conclusion is given about the whole study.

2 Governing equations

The basic equations (PDEs) which govern the continuous motion of a perfectly conducting fluid, in the absence of viscosity and thermal conduction, can be written as [35]:

$$\rho_{t} + div (\rho u) = 0,$$

$$u_{t} + (\mathbf{u}.\nabla)\mathbf{u} = -\frac{1}{\rho}\nabla p + (\nabla \times \mathbf{H}) \times \mathbf{B},$$

$$p_{t} + \mathbf{u}.\nabla p + \rho C^{2}\nabla .\mathbf{u},$$

$$B_{t} = curl (\mathbf{u} \times \mathbf{B}),$$

$$div (\mathbf{B}) = 0.$$
(2.1)

where ρ is the fluid density, p the pressure, C the speed of sound, $\mathbf{u} = (u1, u2, u3)$ the velocity vector and B the magnetic induction satisfying the relation $\mathbf{B} = \mu \mathbf{H}$ with μ being the magnetic permeability, assumed to be constant, and $\mathbf{H} = (H1, H2, H3)$ being the magnetic field vector.

Here, we are concerned with a one-dimensional motion with planar symmetry, which is encountered very frequently in problems of magnetohydrodynamics. In a planar motion, the trajectories of the particles form a family of straight lines perpendicular to some fixed plane. If we choose the x-axis perpendicular to the plane, then the velocity vector will have only one non-zero component, that is, $\mathbf{u} = (u(x, t), 0, 0)$, while p = p(x, t) and $\rho = \rho(x, t)$. We now consider a one-dimensional planar motion of plasma, which is assumed to be an ideal polytropic dusty gas with infinite electrical conductivity and to be permeated by a transverse magnetic field $\mathbf{H} = (0, H(x, t), 0)$ orthogonal to the trajectories of the gas particles; the governing equations for the one-dimensional flow, thus, take the form

$$\rho_t + \nu \rho_x + \rho \nu_x = 0, \tag{2.2}$$

$$v_t + vv_x + \frac{1}{\rho} \left(p_x + \frac{BB_x}{\mu} \right) = 0,$$
 (2.3)

$$p_t + vp_x + C^2 \rho v_x = 0,$$
 (2.4)

$$B_t + \nu B_x + B\nu_x = 0. {(2.5)}$$

The equation of state for a polytropic dusty gas is given as [30]

$$p = ke^{S/c_{\nu}} \left(\frac{\rho}{1 - Z}\right)^{\Gamma}, \tag{2.6}$$

where k is a positive constant and S denotes the specific entropy. Here, $Z = \frac{V_{sp}}{V_{mix}}$ denotes the volume fraction where V_{sp} is the volumetric extension of the solid particles and V_{mix} is the total volume of the mixture, respectively. Γ is the Gruneisen coefficient and defined as $\Gamma = \gamma \frac{(1+\lambda \phi)}{1+\lambda \phi y}$, with $\lambda = \frac{K_p}{(1-K_p)}$, $\gamma = c_p/c_v$, $\phi = c_{sp}/c_p$. Here, $K_p = \frac{k_{sp}}{k_{mix}}$ denotes the mass fraction of the solid particles in the mixture where K_{sp} and k_{mix} are the total mass of the solid particles and the mixture, respectively, c_p is the specific heat of the gas at constant pressure, c_{sp} represents the specific heat of the solid particles and c_{ν} represents the specific heat of the gas at constant volume. The relation between Z and K_p is given as $Z = \theta \rho$ with $\theta = K_p/\rho_{sp}$, ρ_{sp} represents the specific density of the solid particles. For an ideal polytropic dusty gas

medium, the sound velocity $C = \left(\frac{\Gamma_p}{\rho(1-\theta p)}\right)^{1/2}$.

The internal energy per unit mass of the mixture is denoted by e and given as

$$e = \frac{p(1-Z)}{\rho(\Gamma-1)}. (2.7)$$

Eqs. (2.2)–(2.5) can be represented in the matrix form as

$$V_t + AV_x = 0, (2.8)$$

where

$$V = \begin{bmatrix} \rho \\ v \\ p \\ B \end{bmatrix}, \quad A = \begin{bmatrix} v & \rho & 0 & 0 \\ 0 & v & \frac{1}{\rho} & \frac{B}{\mu \rho} \\ 0 & \rho C^2 & v & 0 \\ 0 & B & 0 & v \end{bmatrix}$$

The eigenvalues of the matrix A are obtained as

$$\lambda_1 = \nu - s, \ \lambda_2 = \nu, \ \lambda_3 = \nu + s, \ \lambda_4 = \nu, \tag{2.9}$$

where $s = (b^2 + C^2)^{1/2}$ is magneto-acoustic speed, $b = \sqrt{\frac{B^2}{\mu o}}$ is the Alfvén speed.

The eigenvectors corresponding to the eigenvalues λ_i , j = 1, 2, 3, 4 of matrix A are

$$X_{1} = \begin{bmatrix} \rho/s \\ 1 \\ \rho s \\ 0 \end{bmatrix}, \quad X_{2} = \begin{bmatrix} 1 \\ 0 \\ 0 \\ 0 \end{bmatrix}, \quad X_{3} = \begin{bmatrix} -\rho/s \\ 1 \\ -\rho s \\ 0 \end{bmatrix}, \quad X_{4} = \begin{bmatrix} 1 \\ 0 \\ -b^{2} \\ 1 \end{bmatrix}. \quad (2.10)$$

Since the eigenvalues of the matrix A are real, and the corresponding set of eigenvectors are linearly independent. So, the system (2.8) is hyperbolic. Now, we impose an assumption $B = k\rho$ (see Refs. [35, 36]), where k is a positive constant. With this assumption Eq. (2.2) is equivalent to Eq. (2.5). Hence, the system (2.5) reduces to the simpler form as follows:

$$V_t^* + A^* V_y^* = 0, (2.11)$$

where

$$V^* = \begin{bmatrix} \rho \\ \nu \\ p \end{bmatrix}, \quad A^* = \begin{bmatrix} \nu & \rho & 0 \\ \frac{b^2}{\rho} & \nu & \frac{1}{\rho} \\ 0 & \rho C^2 & \nu \end{bmatrix}$$

Since the eigenvalues of A^* are real and distinct for s > 0, therefore the system (2.11) is strictly hyperbolic. The eigenvectors of A^* are given as

$$X_1^* = \begin{bmatrix} -\rho/s \\ 1 \\ \rho C^2/s \end{bmatrix}, \quad X_2^* = \begin{bmatrix} 1 \\ 0 \\ -b^2 \end{bmatrix}, \quad X_3^* = \begin{bmatrix} \rho/s \\ 1 \\ \rho C^2/s \end{bmatrix}.$$
 (2.12)

3 The Riemann problem and the generalized Riemann invariants

The conservative form of (2.11) can be written as

$$\frac{\partial V^*}{\partial t} + \frac{\partial F(V^*)}{\partial x} = 0, \tag{3.1}$$

where $V^* = (\rho, \rho v, (E + B^2/\mu \rho))^{tr}, F(V^*) = (\rho v, p + \rho v^2 + (B^2/\mu \rho))^{tr}, V(E + p + B^2/2\mu))^{tr}$ with $E = \rho e + \frac{\rho v^2}{2}$.

The Riemann problem for the system (3.1) is an initial value problem with the following initial data

$$V_{r,0}^* = V_0^*(r) = \begin{cases} V_l^*, & x < 0, \\ V_r^*, & x > 0, \end{cases}$$
(3.2)

where V_l^* and V_r^* are left and right constant states, respectively which are separated by a jump discontinuity at the point x=0. The solution of the Riemann problem (3.1) and (3.2) has three waves associated with distinct eigenvalues. Since, all the characteristic fields of the system (2.11) are either linearly degenerate for $\nabla \lambda_j X^j = 0$ or genuinely non-linear according for $\nabla \lambda_j X^j \neq 0$. Hence, first and third characteristic fields are genuinely non-linear while second characteristic field is linearly degenerate. So, the first and third characteristic fields will always be either a shock or rarefaction wave, and the second characteristic field will be contact discontinuity.

Now, we consider the matrix $M_{3\times3}$ whose columns are eigenvectors X_i^* , j=1,2,3 as

$$\begin{bmatrix} -\rho/s & 1 & \rho/s \\ 1 & 0 & 1 \\ -\rho C^2/s & -b^2 & \rho C^2/s \end{bmatrix}.$$

The inverse of the above matrix is given as

$$\begin{bmatrix} \frac{1}{\chi^2} & 0 & \frac{-1}{C^2\chi^2} \\ \frac{-C(\chi^2 - 1)}{2\rho\chi} & \frac{1}{2} & \frac{-1}{2C\rho\chi} \\ \frac{C(\chi^2 - 1)}{2\rho\chi} & \frac{1}{2} & \frac{1}{2C\rho\chi} \end{bmatrix}$$

Here, $\chi = (1 + b^2/C^2)^{1/2}$ denotes Alfvèn number. Now, we try to integrate

$$\frac{1}{\chi^{2}}d\rho - \frac{1}{C^{2}\chi^{2}}dp, \quad \left(\frac{1}{\chi} - \chi\right)\frac{C}{\rho}d\rho + du - \frac{1}{C\rho\chi}dp,$$

$$\left(\chi - \frac{1}{\chi}\right)\frac{C}{\rho}d\rho + du + \frac{1}{C\rho\chi}dp.$$
(3.3)

The first differential of (3.3) can be written as

$$\frac{1}{\chi^2}d\rho - \frac{1}{C^2\chi^2}dp = \frac{\left(1 - \theta\rho\right)}{\chi^2}d\left(\frac{\left(\rho/\left(1 - \theta\rho\right)\right)^{\Gamma}}{p}\right),$$

which implies that the entropy $S = \frac{p}{(\rho/(1-\theta\rho))^T}$ is constant along the particle path through smooth solutions. From the entropy condition and the remaining two differentials in (3.3), we obtain the following relations:

$$R^{\pm} = \nu \pm \frac{2\chi C}{(\Gamma - 1)} (1 - \theta \rho)^{1/2}.$$
 (3.4)

Therefore, the Riemann invariants (Π_1^i, Π_2^i) corresponding to the *i*th-characteristic field are given as

$$i = 1, \ \Pi_1^1 = S, \ \Pi_2^1 = \nu + \frac{2\chi C}{(\Gamma - 1)} (1 - \theta \rho)^{1/2},$$
 (3.5)

$$i = 2$$
, $\Pi_1^2 = u$, $\Pi_2^2 = p + \frac{B^2}{2u}$, (3.6)

$$i = 3$$
, $\Pi_1^1 = S$, $\Pi_2^1 = \nu - \frac{2\chi C}{(\Gamma - 1)} (1 - \theta \rho)^{1/2}$. (3.7)

4 Shock waves

Shock waves are the piecewise discontinuous solutions, which satisfy the Lax entropy condition. Let us suppose that the shock propagates at a velocity σ , dependent on the left and right constant states. The conserved variables must satisfy the R-H relations [37]. Let V_1^* and V_2^* represent the left and right constant states, respectively separated by either a shock or simple wave or contact discontinuity i. e.,

$$F(V_2^*) - F(V_1^*) = \sigma(V_2^* - V_1^*). \tag{4.1}$$

Thus, we have the following jump relations of the system (3.1)

$$\sigma[\rho] = [\rho \nu], \tag{4.2}$$

$$\sigma[\rho v] = [p + \rho v^2 + (B^2/2\mu)], \tag{4.3}$$

$$\sigma[e + (B^2/2\mu)] = [v(e + p + (B^2/2\mu))]. \tag{4.4}$$

The Lax entropy condition is as follows [38]:

$$\lambda_{i-1}(V_1^*) < \sigma < \lambda_i(V_1^*), \ \lambda_i(V_2^*) < \sigma < \lambda_{i+1}(V_2^*), \ i = 1, 3.$$
 (4.5)

By introducing the variables $u = v - \sigma$, $m = \rho u$ in the above jump conditions, we have

$$[m] = 0, \tag{4.6}$$

$$[p + mu + (B^2/2\mu)] = 0,$$
 (4.7)

$$m\left[u^2 + \frac{2}{\Gamma(\Gamma - 1)}C^2(1 - \theta\rho)(\Gamma - \theta\rho) + b^2\right] = 0.$$
 (4.8)

Using Eq. (4.5) for 1-shock waves, we obtain $\sigma < v_1 - s_1$, which implies $s_1 < u_1$ and $v_2 - s_2 < \sigma < v_2$, which imply $0 < u_2 < s_2 < u_2 + \sigma$. Therefore, in case of 1-shock wave, we have $u_1 > s_1$ and $0 < u_2 < s_2$, which imply that $v_1 > \sigma$ and $v_2 > \sigma$. Thus, the gas velocity is greater than the shock velocity on both sides of the shock wave, so that for a 1-shock, particles move from left to right across the shock. For 3shock wave, we have $v_1 < \sigma < v_1 + s_1$ and $v_2 + s_2 < \sigma$, which imply that $-s_1 < u_1 < 0$ and $u_2 < -s_1 < 0$. Therefore, for 3shock wave, we obtain $\sigma > v_1$ and $\sigma > v_2$, which imply that the shock velocity is greater than the velocity of gas on both sides of the shock wave. So, the particles move across the 3shock from right to left.

It can be noticed that u_1 and u_2 are non-zero for 1-shock wave and 3-shock wave. Therefore, $m = \rho_1 u_1 = \rho_2 u_2 \neq 0$. Thus, for both the shock waves, we have $u_1^2 > s_1^2$ and $u_2^2 < s_2^2$. Since $m \neq 0$, so from the Eq. (4.7), we obtain the following relation

$$u_1^2 + \frac{2}{\Gamma(\Gamma - 1)} C_1^2 (1 - Z_1) (\Gamma - Z_1) + b_1^2 = u_2^2 + \frac{2}{\Gamma(\Gamma - 1)} C_2^2 (1 - Z_2) (\Gamma - Z_2) + b_2^2,$$
(4.9)

where $Z_1 = \theta \rho_1$ and $Z_2 = \theta \rho_2$.

Now, using the fact that $u_1^2 > s_1^2$ and $u_2^2 < s_2^2$ in Eq. (4.9), we obtain

$$s_{1}^{2} + \frac{2}{\Gamma(\Gamma - 1)}C_{1}^{2}(1 - Z_{1})(\Gamma - Z_{1}) + b_{1}^{2} < s_{2}^{2} + \frac{2}{\Gamma(\Gamma - 1)}C_{2}^{2}(1 - Z_{2})(\Gamma - Z_{2}) + b_{2}^{2}.$$

$$(4.10)$$

Substituting $s^2 = (b^2 + C^2)$ in the above equation, we get $C_1^2 < C_2^2$ and $b_2^2 < b_2^2$ which implies that $s_1^2 < s_2^2$ thus $u_1^2 > u_2^2$. This gives $s_2 > s_1$ and $|u_1| > |u_2|$. Therefore, from Eq. (4.6), we obtain $\rho_1 < \rho_2$, so $p_1 < p_2$ and $B_1 < B_2$ for 1-shock wave. In a similar manner, we can prove that $\rho_2 < \rho_1$, $p_2 < p_1$ and $B_2 < B_1$ for 3-shock wave. Hence, both the shock families are compressive waves.

Now, we explicitly compute the one-parameter family of shocks. We start with 1-shock wave and define the following constants:

$$\pi = \frac{p_2}{p_1}, \ \alpha = \frac{\rho_2}{\rho_1}, \ \tau = \frac{(\Gamma + 1)}{(\Gamma - 1)}, \ \beta = \frac{(\Gamma - 1)}{2\Gamma}.$$
 (4.11)

The above relations shows that $\pi > 1$ and $\alpha > 1$. Using the relation $C^2 = \frac{\Gamma p}{\alpha(1-Z)}$, we get

$$\left(\frac{C_2}{C_1}\right)^2 = \frac{\pi}{\alpha} \frac{(1 - Z_1)}{(1 - Z_2)}.$$
 (4.12)

With the help of $\rho_1 u_1 = \rho_2 u_2$, we get

$$\frac{u_2}{u_1} = \frac{\rho_1}{\rho_2} = \frac{1}{\alpha}.$$
 (4.13)

Using Eqs. (4.12) and (4.13) in Eq. (4.9), we obtain

$$\left(\frac{u_1}{C_1}\right)^2 = \left[2(1-Z_1)\frac{\pi(1-Z_2) - \alpha(\Gamma-Z_1)}{\Gamma(\Gamma-1)} + \frac{\pi(1-Z_1)(\chi_2^2-1)}{(1-Z_2)} - \alpha(\chi_1^2-1)\right] \frac{\alpha}{\alpha^2-1}.$$
(4.14)

Here, $\chi_1 = (1 + b_1^2/C_1^2)^{1/2}$ and $\chi_2 = (1 + b_2^2/C_2^2)^{1/2}$ Also, from Eq. (4.7), we have

$$p_1 + m_1 u_1 + (B_1^2/2\mu) = p_2 + m_2 u_2 + (B_2^2/2\mu).$$
 (4.15)

Since $p = \rho C^2 (1 - Z)/\Gamma$, $m = \rho u$ and $B^2/\mu \rho = b^2$, therefore Eq. (4.15) yields

$$\left(\frac{u_1}{C_1}\right)^2 = \left[\frac{(1-Z_1)(\pi-1)}{\Gamma} + \frac{1}{2} \left\{\frac{\pi(1-Z_1)(\chi_2^2-1)}{(1-Z_2)} - (\chi_1^2-1)\right\}\right] \frac{\alpha}{\alpha-1}.$$
(4.16)

Comparing Eqs. (4.14) and (4.16), we obtain

$$\alpha = \frac{\frac{1}{\Gamma} \left(1 + \pi \tau - \frac{2\pi Z_2}{\Gamma - 1} \right) + K}{\frac{1}{\Gamma} \left(\pi + \tau - \frac{2Z_1}{\Gamma - 1} \right) + K},$$
(4.17)

where
$$K = \frac{1}{2} \left[\frac{\pi(\chi_2^2 - 1)}{1 - Z_2} + \frac{(\chi_1^2 - 1)}{(1 - Z_1)} \right]$$
.

Above equation implies $\alpha < \tau$ and since $1 < \alpha$, we find the bounds for the density ρ_2 in terms of ρ_1 i. e., $\rho_1 < \rho_2 < \tau \rho_1$.

Substituting the value of α from Eq. (4.17) in Eq. (4.16), we obtain

$$\left(\frac{u_{1}}{C_{1}}\right)^{2} = \left[\frac{(1-Z_{1})(\pi-1)}{\Gamma} + \frac{1}{2} \left\{\frac{\pi(1-Z_{1})(\chi_{2}^{2}-1)}{(1-Z_{2})} - (\chi_{1}^{2}-1)\right\}\right] \frac{\frac{1}{\Gamma}\left(1+\pi\tau-\frac{2\pi Z_{2}}{\Gamma-1}\right) + K}{\frac{1}{\Gamma}\left\{(\pi-1)(1-\tau) - \frac{2(\pi Z_{2}-Z_{1})}{\Gamma-1}\right\} + K}.$$
(4.18)

Let $\eta = \frac{2Z_1}{\Gamma - 1}$, $\xi = \frac{2Z_2}{\Gamma - 1}$ and using $u = v - \sigma$ in Eq. (4.18), we

$$\frac{\nu_2-\nu_1}{C_1}=\pm\left[\frac{\left(2-\eta\left(\Gamma-1\right)\right)}{2}\left\{\frac{1-\pi}{\Gamma}-\frac{\pi\left(\chi_2^2-1\right)}{2-\xi\left(\Gamma-1\right)}-\frac{\left(\chi_1^2-1\right)}{2-\eta\left(\Gamma-1\right)}\right\}$$

$$\frac{\left((1-\pi)(\tau-1) - \eta + \pi \xi \right)}{\left(1 + \pi(\tau-\xi) \right)} \bigg|^{1/2}.$$
 (4.19)

Eq. (4.19) shows the change in velocity across a shock transition. Here, + sign denoted for 1-shock and sign for 3-shock.

The expressions $\frac{p_2}{p_1} = \pi$ and $\frac{\rho_2}{\rho_1} = \alpha$ together with Eqs. (4.17) and (4.19) give the formulas for the shock curves. To make these somewhat more explicit, we introduce a new parameter δ as follows [39]:

$$\delta = -\log \pi. \tag{4.20}$$

From the above equation, we have $e^{-\delta} = \pi = p_2/p_1 > 1$, therefore $\delta \leq 0$. By using this parameterization, we obtain the following formulas for 1-shock curve

$$\frac{p_2}{p_1} = e^{-\delta},$$
 (4.21)

$$\frac{\rho_2}{\rho_1} = \frac{\frac{\left(\chi_1^2 - 1\right)}{2} + \frac{e^{-\delta}(1 - Z_1)\left(\chi_2^2 - 1\right)}{2(1 - Z_2)} + \frac{(1 - Z_1)\left(1 + e^{-\delta}\left(\tau - \xi\right)\right)}{\Gamma}}{\frac{\left(\chi_1^2 - 1\right)}{2} + \frac{e^{-\delta}(1 - Z_1)\left(\chi_2^2 - 1\right)}{2(1 - Z_1)} + \frac{(1 - Z_1)\left(\tau - \eta + e^{-\delta}\right)}{\Gamma}},\tag{4.22}$$

$$\frac{\nu_{2} - \nu_{1}}{C_{1}} = \left[\frac{\left(2 - \eta \left(\Gamma - 1\right)\right)}{2} \left\{ \frac{1 - e^{-\delta}}{\Gamma} - \frac{e^{-\delta} \left(\chi_{2}^{2} - 1\right)}{2 - \xi \left(\Gamma - 1\right)} - \frac{\left(\chi_{1}^{2} - 1\right)}{2 - \eta \left(\Gamma - 1\right)} \right\} \\
- \frac{\left(\left(1 - e^{-\delta}\right)\left(\tau - 1\right) - \eta + \pi \xi\right)}{\left(1 + e^{-\delta} \left(\tau - \xi\right)\right)} \right]^{1/2} .$$
(4.23)

Similarly, for 3-shock curve, we have

$$\frac{p_1}{p_2} = e^{\delta},\tag{4.24}$$

$$\frac{\rho_{1}}{\rho_{2}} = \frac{\frac{\left(\chi_{1}^{2}-1\right)}{2} + \frac{e^{\delta}\left(1-Z_{1}\right)\left(\chi_{2}^{2}-1\right)}{2\left(1-Z_{2}\right)} + \frac{\left(1-Z_{1}\right)\left(1+e^{\delta}\left(\tau-\xi\right)\right)}{\Gamma}}{\frac{\left(\chi_{1}^{2}-1\right)}{2} + \frac{e^{\delta}\left(1-Z_{1}\right)\left(\chi_{2}^{2}-1\right)}{2\left(1-Z_{2}\right)} + \frac{\left(1-Z_{1}\right)\left(\tau-\eta+e^{\delta}\right)}{\Gamma}},$$
(4.25)

$$\frac{\nu_{1} - \nu_{2}}{C_{2}} = \left[\frac{\left(2 - \eta(\Gamma - 1)\right)}{2} \left\{ \frac{e^{\delta} - 1}{\Gamma} - \frac{e^{\delta}(\chi_{2}^{2} - 1)}{2 - \xi(\Gamma - 1)} - \frac{(\chi_{1}^{2} - 1)}{2 - \eta(\Gamma - 1)} \right\} - \frac{\left((e^{\delta} - 1)(\tau - 1) - \eta + \pi\xi\right)}{\left(1 + e^{\delta}(\tau - \xi)\right)} \right]^{1/2}.$$
(4.26)

5 Simple waves

In 1-dimensional space, for a system of hyperbolic PDEs, a simple wave is called a centered rarefaction wave in which the dependent variables are constant along the characteristics which are straight lines. For a rarefaction wave, the left and right constant states i. e., V_1^* and V_2^* are connected through a smooth transition in ith genuinely nonlinear characteristic field and agrees with the following conditions:

- "The Riemann invariants are constant across the wave [40]."
- "The left and right characteristics of the wave diverge i. e., $\lambda_i(V_1^*) < \lambda_i(V_2^*)$, i = 1, 3."

Now, we consider the simple wave curves. We obtain only 1-simple waves, the procedure for 3-simple waves are similar. Using the above conditions, we obtain

$$S_2 = S_1,$$
 (5.1)

and

$$v_1 + \frac{2}{(\Gamma - 1)} \chi_1 C_1 (1 - Z_1)^{1/2} = v_2 + \frac{2}{(\Gamma - 1)} \chi_2 C_2 (1 - Z_2)^{1/2}.$$
 (5.2)

From Eqs. (2.6) and (5.1), we obtain

$$\frac{p_2}{p_1} = \left[\frac{C_2 (1 - Z_2)}{C_1 (1 - Z_1)} \right]^{\frac{2\Gamma}{\Gamma - 1}} = \left[\frac{\rho_2 (1 - Z_1)}{\rho_1 (1 - Z_2)} \right]^{\Gamma}.$$
 (5.3)

Therefore, from Eq. (5.2), we obtain

$$\frac{v_2 - v_1}{C_1} = \frac{2\chi_1}{\Gamma - 1} \left[(1 - Z_1)^{1/2} - \frac{C_2}{C_1} \frac{\chi_2}{\chi_1} (1 - Z_2)^{1/2} \right]. \tag{5.4}$$

But in 1-rarefaction wave, $\lambda_1 = v - s$ must increase. Hence, $\lambda_1^{(2)} \ge \lambda_1^{(1)}$ which implies $\nu_2 - \nu_1 \ge \chi_2 C_2 - \chi_1 C_1$.

$$\frac{\chi_2 C_2 - \chi_1 C_1}{C_1} \le \frac{2\chi_1}{\Gamma - 1} \left[(1 - Z_1)^{1/2} - \frac{C_2}{C_1} \frac{\chi_2}{\chi_1} (1 - Z_2)^{1/2} \right]. \tag{5.5}$$

Using the above expression in Eq. (5.3), we obtain

$$0 < \frac{p_2}{p_1} \le 1. \tag{5.6}$$

From Eq. (4.20), we have

$$\delta = -log\pi. \tag{5.7}$$

Note that $e^{-\delta} = \pi = \frac{p_2}{p_1} < 1$, which implies that $\delta \ge 0$. Therefore, using Eqs. (5.2) and (5.3), the more explicit formulation for 1-simple wave can be written as follows:

$$\frac{p_2}{n_1} = e^{-\delta},\tag{5.8}$$

$$\frac{\rho_2}{\rho_1} = e^{-\delta/\Gamma} \left(\frac{1 - Z_2}{1 - Z_1} \right), \tag{5.9}$$

$$\frac{\nu_2 - \nu_1}{C_1} = \frac{2\chi_1}{\Gamma - 1} (1 - Z_1)^{1/2} \left[1 - e^{-\delta\beta} \frac{\chi_2}{\chi_1} \frac{(1 - Z_1)^{1/2}}{(1 - Z_2)^{1/2}} \right].$$
 (5.10)

Similarly, for 3-simple wave, we have

$$\frac{p_1}{p_2} = e^{\delta},\tag{5.11}$$

$$\frac{\rho_1}{\rho_2} = e^{\delta/\Gamma} \left(\frac{1 - Z_1}{1 - Z_2} \right),$$
 (5.12)

$$\frac{\nu_1 - \nu_2}{C_2} = \frac{2\chi_1}{\Gamma - 1} (1 - Z_1)^{1/2} \left[1 - \frac{\chi_2}{\chi_1} e^{\delta \beta} \frac{(1 - Z_1)^{1/2}}{(1 - Z_2)^{1/2}} \right].$$
 (5.13)

6 Contact discontinuities

The contact surfaces that separate two zones of different temperature and density are called contact discontinuities. Contact discontinuity comes due to the linear degeneracy of the second characteristics field. In this field, there are no shocks or simple waves. For this type of discontinuity, the constant states V_1^* and V_2^* are joined through a single jump discontinuity with the speed σ_2 and satisfying the following conditions:

- "The Rankine-Hugoniot (R-H) conditions i. e., $F(V_2^*) - F(V_1^*) = \sigma_2(V_2^* - V_1^*)$."
- "The parallel characteristic conditions $\lambda_2(V_2^*) = \lambda_1$

Thus, for the 1-parameter family of contact discontinuities,

$$\frac{p_2}{p_1} = 1,$$
 (6.1)

$$\frac{\rho_2}{\rho_1} = e^{\delta}, -\infty < \delta < \infty, \tag{6.2}$$

$$v_2 - v_1 = 0. ag{6.3}$$

7 Results and discussion

The analytical solutions of the Riemann problem (shock waves, simple waves and contact discontinuities) for Euler equations in magnetogasdynamics of an ideal polytropic dusty gas are determined. The case when $k_p = 0$, corresponds to the ideal polytropic gas in magnetogasdynamics without the presence of dust particles. The obtained results for this case are in close agreement with the earlier results reported in [41] for an ideal gas with added magnetic field effect. The case for which $\chi_1 = 1.0$, $\chi_2 = 1.0$, $k_p \neq 0$ in the expressions of 1-shock and 3-shock for compressive and rarefaction waves corresponds to the case of ideal polytropic dusty gas without magnetic field effects and the obtained solutions for this case perfectly match with the existing results reported in [30]. Further, in the absence of magnetic field and dust particles i. e., $\chi_1 = 1.0$, $\chi_2 = 1.0$,

 $k_p = 0$, the obtained results are in close agreement with the results reported by Smoller [2] for ideal gas dynamics. The velocity and density profiles for 1-shock and 3-shock of compressive and rarefaction waves are plotted in Figures 1–8 for different values of parameters of mass fraction k_n and the magnetic field strength. The density and velocity profiles for compressive and rarefaction waves for 1-shock and 3-shock versus δ are presented for different values of parameters of dusty gas and magnetic field strength in Figures 1–8. Computed values of the density for compressive waves of 1-shock and 3-shock which are obtained in Eqs. (4.22) and (4.25), respectively are presented in Figures 1 and 2, respectively. Similarly, the computed values of the velocity for compressive waves of 1-shock and 3-shock obtained in (4.23) and (4.26), respectively are presented in Figures 3 and 4, respectively. The density profiles of rarefaction waves for 1-shock and 3-shock which are obtained in (5.9) and (5.12), respectively are plotted in Figures 5 and 6, respectively. Similarly, the velocity profiles of rarefaction waves for 1-shock and 3-shock obtained in (5.10) and (5.13), respectively are plotted in Figures 7 and 8, respectively. For obtaining the profiles of compressive and rarefaction waves for 1-shock, the initial data is taken as $p_1 = 1.0$, $u_1 = 0.0$, $\rho_1 = 1.0$, and for the velocity and density profiles of compressive and rarefaction waves for 3-shock, the initial data is taken as $p_2 = 0.1$, $u_2 = 0.0$, $\rho_2 = 0.125$ [35]. All the computations are performed using the software package MATHEMATICA.

For computational work, the following values of the constants are taken

$$Z_1 = 0.03$$
, $Z_2 = 0.04$, $\gamma = 1.4$, $\phi = 0.0$, 0.5, 0.8, 1.0, $k_p = 0.0$, 0.2, 0.3, 0.4

The values $\phi = 1$ and y = 1.4 correspond to the mixture of air and glass particles [31]. The effect of the magnetic field enters through the parameters χ_1 and χ_2 into the solution. Figures 1-8 represent the density and velocity profiles of compressive and rarefaction waves for 1-shock and 3-shock for different values of the parameters of magnetic field strength and mass fraction. While Figures 9-16 represent the density and velocity profiles of compressive and rarefaction waves for 1-shock and 3-shock for different values of ϕ . From Figures 1, 2, 5, and 6 it is observed that the density profiles for both the compressive and rarefaction wave (i. e., 1-shock and 3-shock) are concave upward in nature. Figures 3 and 4 show that velocity profiles of compressive wave are concave upward for 1-shock and concave downward for 3-shock, respectively. For a 1-shock of compressive wave, we observe that an increase in the value of magnetic field strength causes a

decrease in density (Figure 1). In contrast for a 3-shock of compressive wave, the density increases with an increase in the value of magnetic field strength (Figure 2). This result closely agrees with the result obtained in [10] for the case of a non-ideal gas. An increase in the parameters χ_1 and χ_2 gives rise in the velocity for both the compressive waves as well as rarefaction waves (1-shock and 3-shock). Further, an increment in the value of the parameter k_n gives a rise in the velocity and density for 1-shock of compressive wave and the same effect of k_p causes a decrement in the velocity and density profiles for 3-shock of compressive wave. It may be noted here that an increase in the value of the parameter k_p causes a decrement in the density of rarefaction waves for 1-shock while for 3-shock of rarefaction waves, the velocity increases with an increment in the value of k_p (see Figures 5 and 6). From Figure 7, it is observed that as the value of k_p increases, the velocity for 1shock of rarefaction wave increases. On the other hand, as

the value of k_p increases in the absence of magnetic field, the velocity increases while the velocity decreases as the value of k_p increases (Figure 8) in the presence of magnetic field. From Figures 9 and 10, it is observed that as we increase the value of parameter ϕ , the density increases for a 1shock of compressive wave, while for a 3-shock, the density decreases. An increment in the value of ϕ gives rise in the velocity of a compressive wave for 3-shock (Figure 12). For rarefaction waves, the density decreases for 1-shock and increases for 3-shock with an increment in the value of ϕ (Figures 13 and 14). Therefore, the effect of dusty gas is to magnify the effect of magnetic field strength further. Thus, it may be concluded from the Figures 1-16 that the presence of the magnetic field and the dust particles affect significantly the solution of the Riemann problem. On the basis of all the results shown in Figures 1-8, it may be concluded that our results are in good agreement when compared with the results reported in [2, 10, 30].

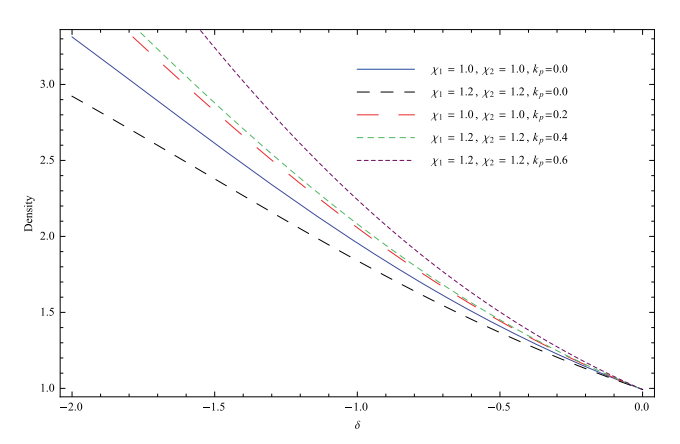


Figure 1: Profiles of density for compressive waves: 1-shock for $\phi = 0.8$.

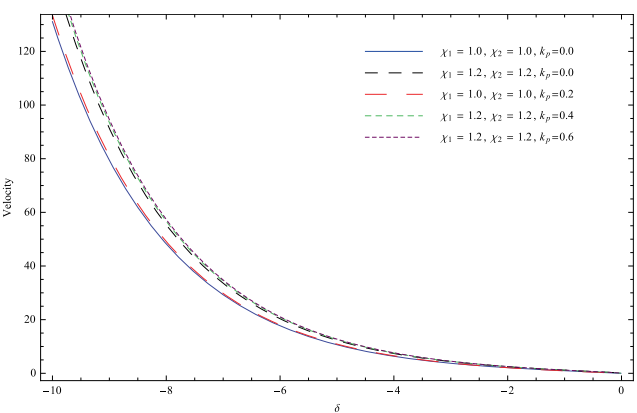


Figure 3: Profiles of velocity for compressive waves: 1-shock for $\phi = 0.8$.

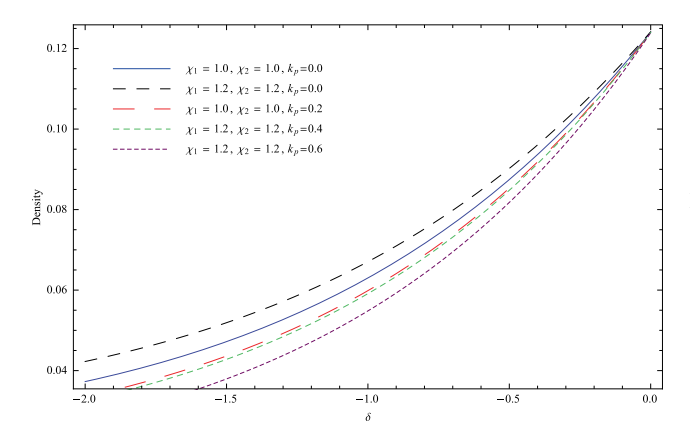


Figure 2: Profiles of density for compressive waves: 3-shock for $\phi = 0.8$.

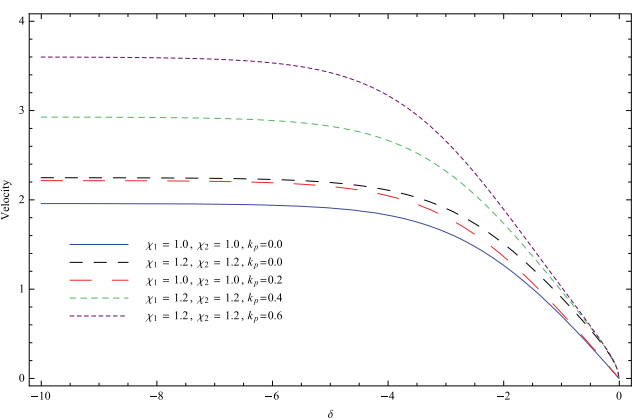


Figure 4: Profiles of velocity for compressive waves: 3-shock for $\phi = 0.8$.

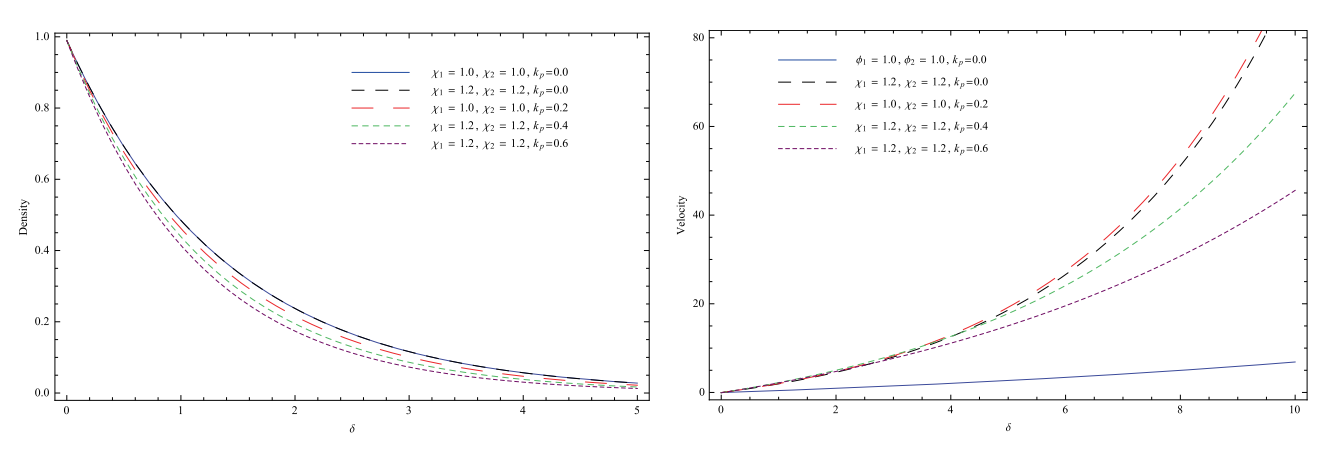


Figure 5: Profiles of density for rarefaction waves: 1-shock for $\phi = 0.8$.



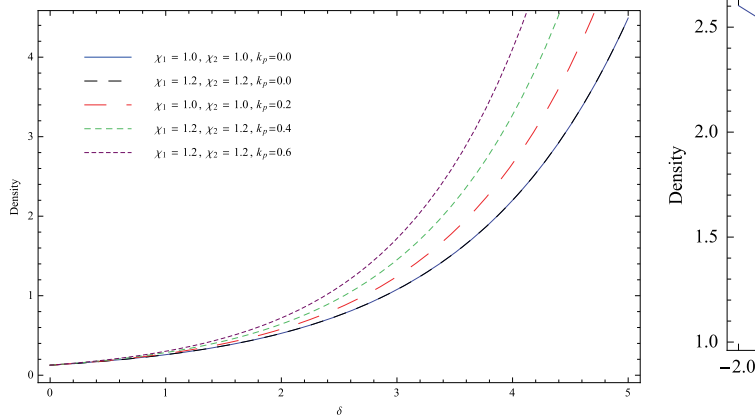


Figure 6: Profiles of density for rarefaction waves: 3-shock for $\phi = 0.8$.

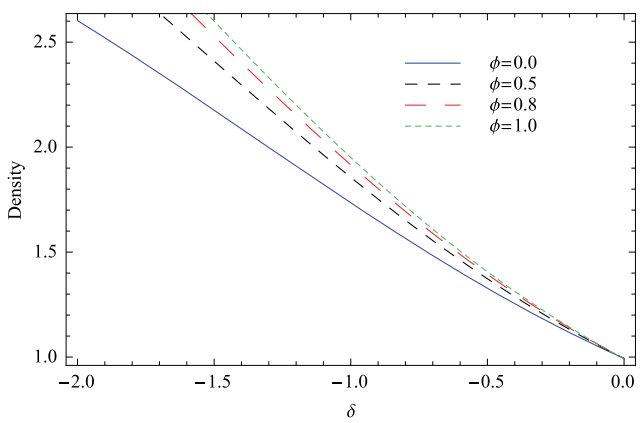


Figure 9: Profiles of density for compressive waves: 1-shock for $k_p = 0.3$, $\chi_1 = 1.4$ and $\chi_2 = 1.4$.

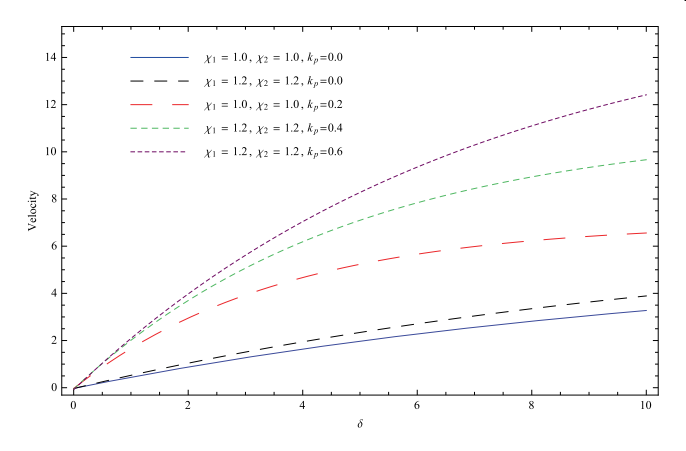


Figure 7: Profiles of velocity for rarefaction waves: 1-shock for $\phi = 0.8$.

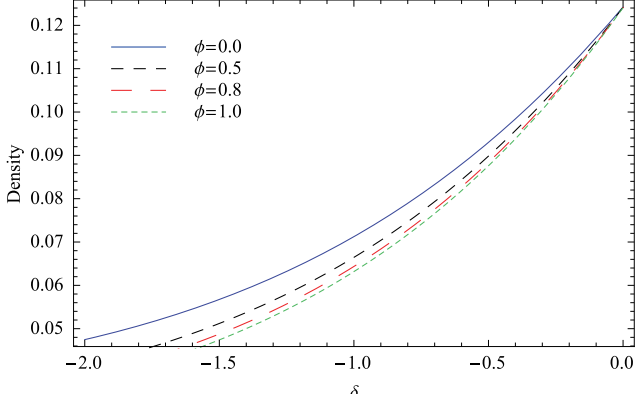


Figure 10: Profiles of density for compressive waves: 3-shock for $k_p = 0.3$, $\chi_1 = 1.4$ and $\chi_2 = 1.4$.

8 Conclusion

In this article, the analytical solution of the Riemann problem is presented for the system of quasi-linear hyperbolic differential equations for an ideal polytropic dusty gas in magnetogasdynamics. It is observed that for a dusty gas, the solution expressions are more complex in

comparison with the corresponding non-magnetic and ideal gas case. In the limit of a vanishing magnetic field, the solutions thus obtained perfectly match with the existing solutions of the Riemann problem for the Euler equations of gas dynamics. Also, it is observed that the obtained results are in good agreement with the earlier

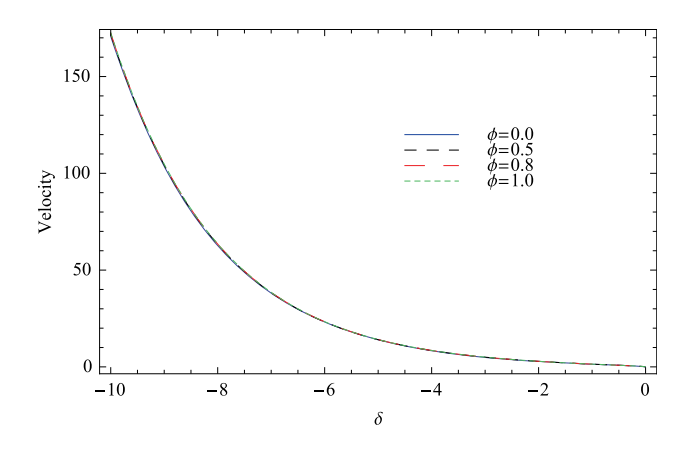


Figure 11: Profiles of velocity for compressive waves: 1-shock for $k_p = 0.3$, $\chi_1 = 1.4$ and $\chi_2 = 1.4$.

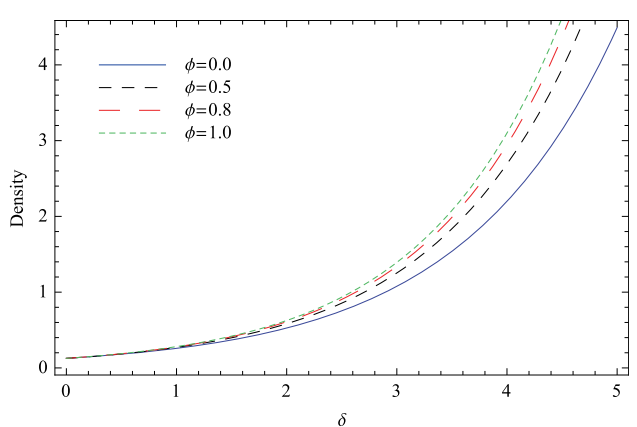


Figure 14: Profiles of density for rarefaction waves: 3-shock for $k_p = 0.3$, $\chi_1 = 1.4$ and $\chi_2 = 1.4$.

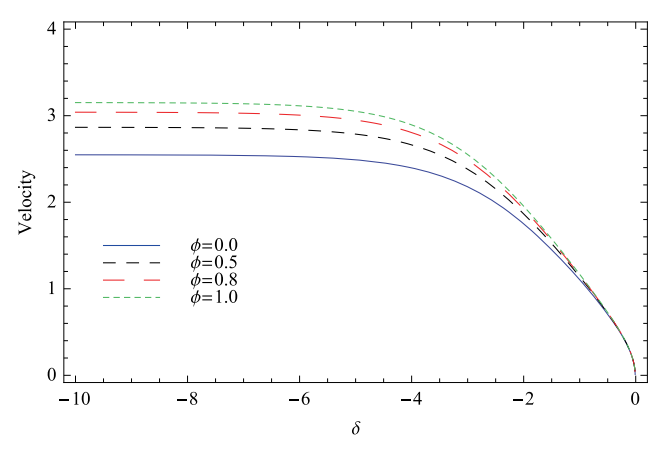


Figure 12: Profiles of velocity for compressive waves: 3-shock for $k_p = 0.3$, $\chi_1 = 1.4$ and $\chi_2 = 1.4$.

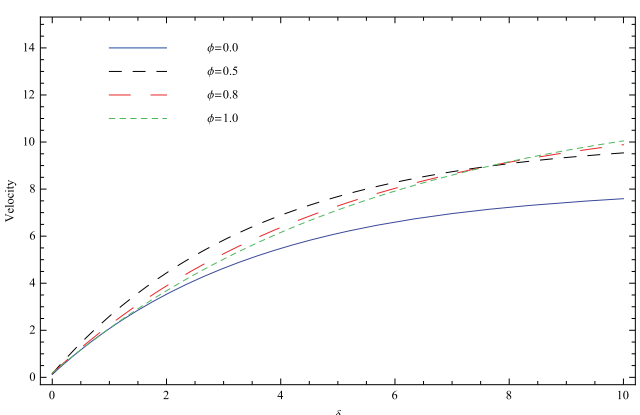


Figure 15: Profiles of velocity for rarefaction waves: 1-shock for $k_p = 0.3$, $\chi_1 = 1.4$ and $\chi_2 = 1.4$.

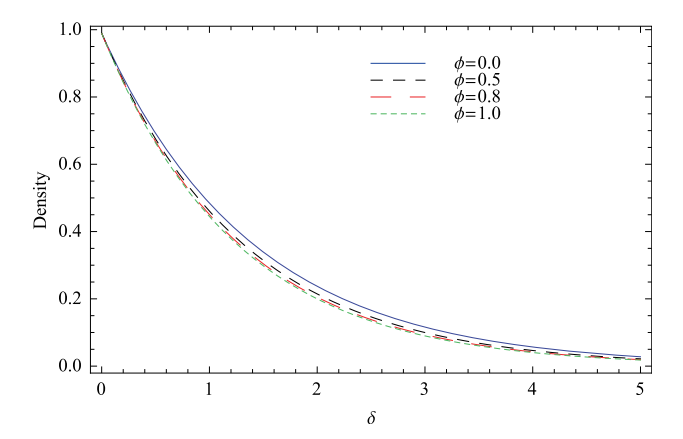


Figure 13: Profiles of density for rarefaction waves: 1-shock for $k_p = 0.3$, $\chi_1 = 1.4$ and $\chi_2 = 1.4$.

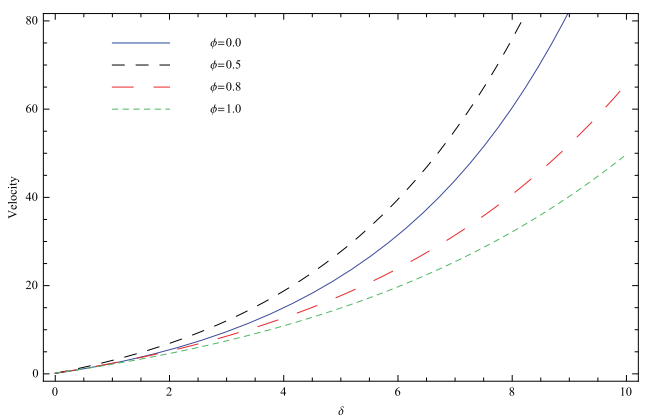


Figure 16: Profiles of velocity for rarefaction waves: 3-shock for $k_p = 0.3$, $\chi_1 = 1.4$ and $\chi_2 = 1.4$.

results reported in the literature for the Euler equations of magnetogasdynamics in an ideal gas without dust particles. The profiles of density and velocity are depicted graphically for compressive and rarefaction waves for 1-shock and 3-shock. Magnetic field strength has a decreasing effect of the density for 1-shock and has an

opposite effect for 3-shock of compressive wave. For compressive waves, the presence of dust particles is to decrease the density for 1-shock and velocity for both shocks i. e., for 1-shock and 3-shock while it has a decreasing effect on the density for 3-shock. For rarefaction waves, the presence of dust particles has an opposite effect on the density as compared to the case of compressive waves.

Funding: The work of the author Astha Chauhan is supported by the "Univ Grant Commission", New Delhi under the senior research fellowship award with grant number "2121440656, Ref. No; 21/12/2014(ii)EU-V."

References

- [1] Richard Courant and Kurt Otto Friedrichs, Supersonic Flow and Shock Waves. Applied Mathematical Sciences, vol. 21, Springer Science & Business Media, 1999.
- [2] J. A. Smoller, "On the solution of the Riemann problem with general step data for an extended class of hyperbolic systems," Mich Math J, vol. 16, no. 3, pp. 201-210, 1969.
- [3] T. Raja Sekhar and V. D. Sharma, 'Riemann problem and elementary wave interactions in isentropic magnetogasdynamics," Nonlinear Anal R World Appl, vol. 11, no. 2, pp. 619-636, 2010.
- [4] Yujin Liu and Wenhua Sun, "Riemann problem and wave interactions in magnetogasdynamics," J Math Anal Appl, vol. 397, no. 2, pp. 454-466, 2013.
- [5] D. Lax Peter, "Hyperbolic systems of conservation laws ii," Commun Pure Appl Math, vol. 10, no. 4, pp. 537-566, 1957.
- [6] Constantine M. Dafermos, "Solution of the Riemann problem for a class of hyperbolic systems of conservation laws by the viscosity method," Arch Ration Mech Anal, vol. 52, no. 1, pp. 1-9, 1973.
- [7] Bruno Giacomazzo and Luciano Rezzolla, "The exact solution of the Riemann problem in relativistic magnetohydrodynamics," J Fluid Mech, vol. 562, pp. 223-259, 2006.
- [8] Roberto Romero, Jose M. Marti, José A. Pons, Jose M. Ibanez, and Juan A. Miralles, "The exact solution of the Riemann problem in relativistic magnetohydrodynamics with tangential magnetic fields," J Fluid Mech, vol. 544, pp. 323-338, 2005.
- [9] K. Ambika and R. Radha, "Riemann problem in non-ideal gas dynamics," Indian J Pure Appl Math, vol. 47, no. 3, pp. 501-521,
- [10] Pooja Gupta, L. P. Singh, and R. Singh, "Riemann problem for non-ideal polytropic magnetogasdynamic flow," Int J Non Lin Mech, vol. 112, 2019. Elsevier.
- [11] Guodong Wang, "The Riemann problem for one dimensional generalized chaplygin gas dynamics," J Math Anal Appl, vol. 403, no. 2, pp. 434-450, 2013.
- [12] Roberto Bernetti, Vladimir A. Titarev, and Eleuterio F. Toro, "Exact solution of the Riemann problem for the shallow water equations with discontinuous bottom geometry," J Comput Phys, vol. 227, no. 6, pp. 3212-3243, 2008.
- [13] Chun Shen, "The Riemann problem for the chaplygin gas equations with a source term," ZAMM-J Appl Math Mech/

- Zeitschrift für Angewandte Mathematik und Mechanik, vol. 96, no. 6, pp. 681-695, 2016.
- [14] D. Zeidan, E. Romenski, Arezki Slaouti, and E. F. Toro. "Numerical study of wave propagation in compressible two-phase flow," Int. J. Numer. Methods Fluid., vol. 54, no. 4, pp. 393-417, 2007.
- [15] D. Zeidan, Arezki Slaouti, E. Romenski, and E. F. Toro. "Numerical solution for hyperbolic conservative two-phase flow equations," Int. J. Comput. Method., vol. 4, no. 02, pp. 299-333, 2007.
- [16] D. Zeidan and R. Touma, "On the computations of gas-solid mixture two-phase flow," Adv. Appl. Math. Mech., vol. 6, no. 1, pp. 49-74, 2014.
- [17] Eric Goncalves and Dia Zeidan, "Simulation of compressible twophase flows using a void ratio transport equation," Commun. Comput. Phys., vol. 24, no. 1, pp. 167-203, 2018.
- [18] D. Zeidan, P. Bähr, P. Farber, J. Gräbel, and P. Ueberholz, "Numerical investigation of a mixture two-phase flow model in twodimensional space," Compu. & Fluid., vol. 181, pp. 90-106, 2019.
- [19] E. Goncalves, Y. Hoarau, and D. Zeidan, "Simulation of shockinduced bubble collapse using a four-equation model," Shock Waves, vol. 29, no. 1, pp. 221-234, 2019.
- [20] S. Kuila and T. Raja Sekhar, "Interaction of weak shocks in driftflux model of compressible two-phase flows," Chaos, Solit. Fractals, vol. 107, pp. 222-227, 2018.
- [21] H. Miura and Irvine Israel Glass, "On the passage of a shock wave through a dusty-gas layer," Proc. Roy. Soc. Lond. Math. Phys. Sci., vol. 385, no. 1788, pp. 85-105, 1983.
- [22] Guillaume Laibe and Daniel J. Price, "Dust and gas mixtures with multiple grain species-a one-fluid approach," Mon. Not. Roy. Astron. Soc., vol. 444, no. 2, pp. 1940-1956, 2014.
- [23] George Rudinger, "Some effects of finite particle volume on the dynamics of gas-particle mixtures," AIAA J., vol. 3, no. 7, pp. 1217-1222, 1965.
- [24] Shih-I. Pai, Two-phase Flows, vol. 3, Springer-Verlag, 2013, https://doi.org/10.1007/978-3-322-86348-5.
- [25] G. Nath and P. K. Sahu, "Self-similar solution of a cylindrical shock wave under the action of monochromatic radiation in a rotational axisymmetric dusty gas," Commun. Theor. Phys., vol. 67, no. 3, pp. 327, 2017.
- [26] Helfried Steiner and Thomas Hirschler, "A self-similar solution of a shock propagation in a dusty gas,". Eur. J.l Mech. Fluid., vol. 21, no. 3, pp. 371-380, 2002.
- [27] P. K. Sahu, "Cylindrical shock waves in rotational axisymmetric non-ideal dusty gas with increasing energy under the action of monochromatic radiation," Phys. Fluid., vol. 29, no. 8, pp. 086102, 2017.
- [28] Meera Chadha and J. Jena, "Wave propagation in a non-ideal dusty gas," Int. J. Non-Linear Mech., vol. 74, pp. 18-24, 2015.
- [29] Astha Chauhan and Rajan Arora, "Self-similar solutions of cylindrical shock wave in a dusty gas," Ind. J. Phys., pp. 1-9, 2019, https://doi.org/10.1007/s12648-019-01499-3.
- [30] Triloki Nath, R. K. Gupta, and L. P. Singh, "Solution of Riemann problem for ideal polytropic dusty gas," Chaos, Solit. Fractals, vol. 95, pp. 102-110, 2017.
- [31] Roy M. Gundersen, Linearized Analysis of One-dimensional Magnetohydrodynamic Flows, vol. 1, Springer Science & Business Media, 2013, https://doi.org/10.1007/978-3-642-46005-0.
- [32] L. P. Singh, R. Singh, and S. D. Ram, "Evolution and decay of acceleration waves in perfectly conducting inviscid radiative magnetogasdynamics," Astrophys. Space Sci., vol. 342, no. 2, pp. 371-376, 2012.

- [33] Roy M. Gundersen, "Magnetohydrodynamic shock wave decay," Zeitschrift für angewandte Mathematik und Physik ZAMP, vol. 40, no. 4, pp. 501-509, 1989.
- [34] Astha Chauhan, Rajan Arora, and Mohd Junaid Siddiqui, "Propagation of blast waves in a non-ideal magnetogasdynamics," Symmetry, vol. 11, no. 4, pp. 458, 2019.
- [35] T. Raja Sekhar and V. D. Sharma, "Solution to the Riemann problem in a one-dimensional magnetogasdynamic flow," Int. J. Comput. Math., vol. 89, no. 2, pp. 200-216, 2012.
- [36] Yanbo Hu and Wancheng Sheng, "The Riemann problem of conservation laws in magnetogasdynamics," Commun. Pure Appl. Anal., vol. 12, no. 2, pp. 755-769, 2013.
- [37] L. Quartapelle, Luigi Castelletti, Alberto Guardone, and Giuseppe Quaranta, "Solution of the Riemann problem of classical

- gasdynamics," J. Comput. Phys., vol. 190, no. 1, pp. 118-140, 2003.
- [38] Peter D. Lax, "Hyperbolic systems of conservation laws ii," Commun. Pure Appl. Math., vol. 10, no. 4, pp. 537-566,
- [39] Joel Smoller, Shock Waves and Reaction-Diffusion Equations, vol. 258, Springer Science & Business Media, 2012, https://doi. org/10.1007/978-1-4612-0873-0.
- [40] Eleuterio F. Toro, Riemann Solvers and Numerical Methods for Fluid Dynamics: A Practical Introduction, Springer Science & Business Media, 2013, https://doi.org/10.1007/b79761.
- [41] R. Singh and L. P. Singh, "Solution of the Riemann problem in magnetogasdynamics," Int. J. Non-Linear Mech., vol. 67, pp. 326-330, 2014.